

Design of End Magnetic Structures for the Advanced Light Source Wigglers*

D. Humphries, J. Akre, E. Hoyer, S. Marks, Y. Minamihara, P. Pipersky, D. Plate, R. Schlueter
Lawrence Berkeley Laboratory, University of California, Berkeley, CA 94720 USA

The vertical magnetic structures for the Advanced Light Source 16 cm planar wiggler and 20 cm period elliptical wiggler are of hybrid permanent magnet design. The ends of these structures are characterized by diminishing scalar potential distributions of the poles which control beam trajectories. They incorporate electromagnetic correction coils to dynamically correct for variations in the first integral of the field as a function of gap. A permanent magnet trim mechanism is incorporated to minimize the transverse integrated error field distribution. The ends were designed using analytic and computer modeling techniques. The design and modeling results are presented.

I. INTRODUCTION

Previous ALS undulators [1] incorporated rotatable permanent magnet tuning elements to adjust the integral of the B_y fields produced by the end magnetic structures. These correctors were adjusted and locked in a fixed setting. Gap dependency of integral B_y for these devices is compensated for by external corrector magnets.

The current ALS wigglers [2] have been designed with electromagnetic end coils which can be dynamically tuned to compensate for gap dependency of integral B_y .

The configuration of the end structure is shown in cross section in Figure 1. The poles, labeled 0, 1, 2, etc. are vanadium permendur and are powered by Nd-Fe-B permanent magnets which can be seen between the poles. The corrector coil can be seen around pole 1. Trim magnets [3] are located between poles 0 and 1. These are used to correct variation in field integrals as a function of the transverse coordinate x .

The truncation field distribution of the ends is a function of the scalar potential distribution of the poles beginning with the end pole (pole 0). The nominal entry scheme is for nominal, normalized scalar potentials of 0, 1/4, -3/4, 1, -1, etc. This distribution is achieved by manipulating the quantities of fixed permanent magnet material in the spaces between poles 0 through 3.

II. CORRECTOR COILS

The corrector coils are powered by a 13 v, 120 A, bi-polar power supply which is controlled by the ALS control system. They consist of ten turns of .250" sq. x .125" i.d. hollow copper conductor potted in glass filled epoxy. They are wired in series to achieve maximum magnetic symmetry with cooling circuits in parallel.

Fluid flow and heat transfer calculations were incorporated in a spread sheet program for rapid optimization of the coil design.

Table I Coil and Power Supply Parameters

Coil Parameters:

Electrical:

Current	100 A
Power	.358 kW
Voltage	3.58 V
Resistance	35.8 m Ω
Inductance	0.5 mH

Cooling:

Velocity	8.79 ft/s
Flow Rate @ 40 psi	.34 GPM
Temperature Rise	4.0° C

Power Supply Requirements:

Output:

Voltage	± 13.0 V
Voltage Ripple (p-p)	<1% V_o
Current	± 120 A
Current Regulation	± 100 ppm
Bipolar Offset	± 25 ppm
Overcurrent	130 A-dc

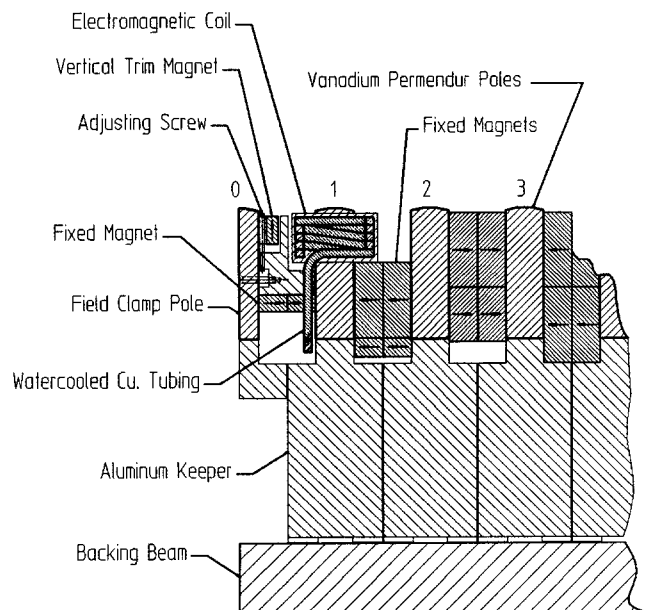


Figure 1: End structure cross section

*This work was supported by the Director, Office of Energy Research, Office of Basic Energy Sciences, Materials Sciences Division, of the U.S. Department of Energy under Contract No. DE-AC03-76SF00098.

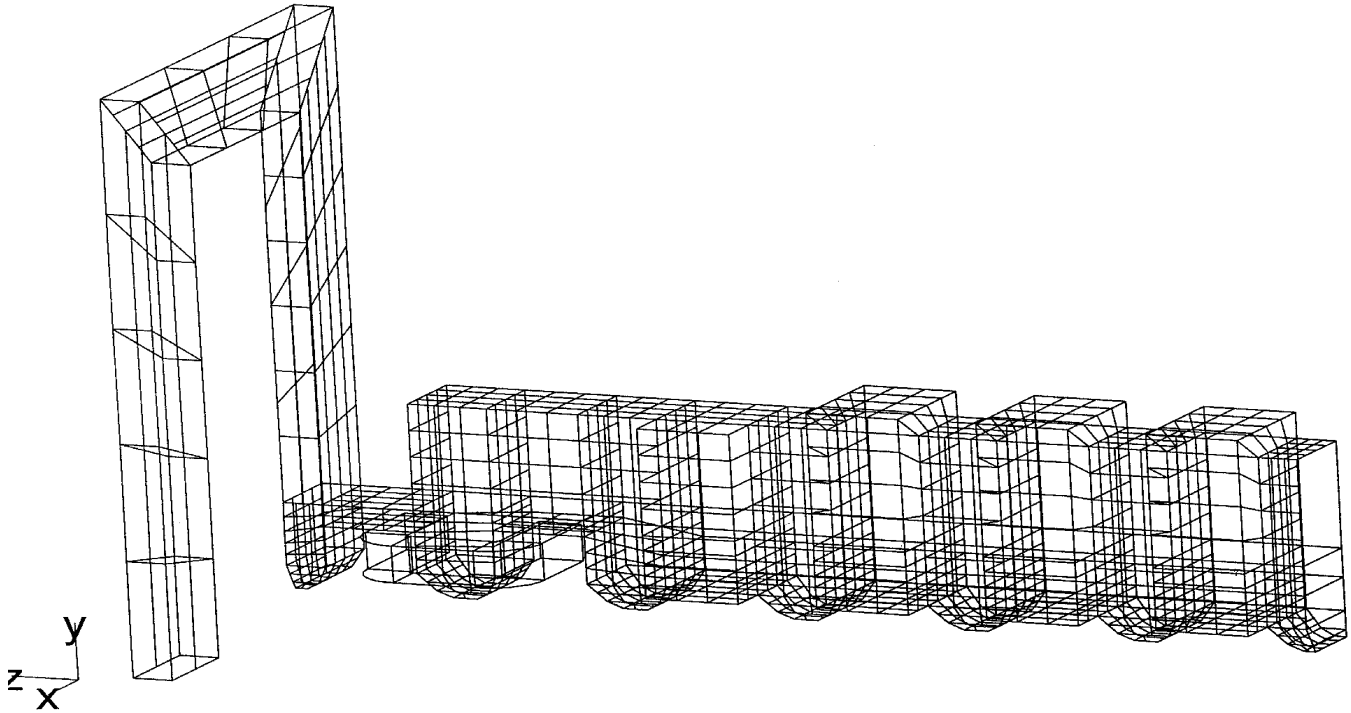


figure 2: 3-D Boundary element model for end field calculations

F

III. 3-D NUMERICAL MODELING

The end structures are complicated, non-linear structures with significant three dimensional aspects. To perform the magnetic design, the code AMPERES [4] was used. AMPERES is a 3-D code which uses a boundary element method to solve for the fields.

Figure 2 illustrates the 3-D model with boundary elements shown. This represents one fourth of one end of the 20 cm wiggler magnetic structure. Symmetry planes are utilized at the $x=0$, $y=0$ and $z=0$ planes of the geometry. One half of one coil can be seen around pole 1.

The poles are modeled using a non-linear B-H curve for vanadium permendur. The permanent magnets are described by the usual linear B-H representation while the coil in the model consists of current volume elements with total current NI.

At the left end of the model in Figure 2, a magnetic shunt can be seen which connects the last or "field clamp" pole to the corresponding pole below the midplane. The intended purpose of this shunt is to force the fields clamp poles to zero scalar potential.

IV. MODELING RESULTS

A. Fields and Trajectories

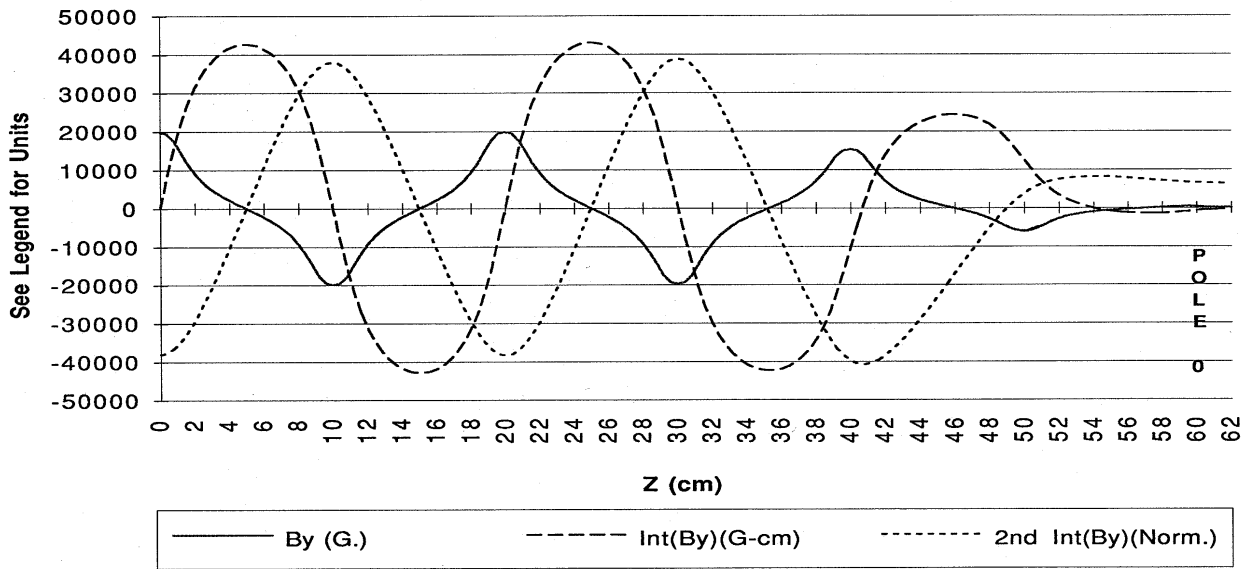
Figure 3 shows a result for the 20 cm wiggler calculated by AMPERES. The B_y field distribution, the first integral of the fields, and the second integral or trajectory are shown.

The high third harmonic content of the wiggler fields can be seen in the shape of the field peaks. Pole 0, the field clamp pole is indicated on the right side of the graph. The first integral of B_y (steering), decays to a small value as desired. The second integral indicates a benign exit trajectory with a final beam offset which is small relative to the wiggler amplitude which can be seen at the left side of the graph.

B. Coil Positioning

3-D calculations were performed with correction coils in various locations in order to determine the optimum arrangement. The results indicate that coils which are positioned further from the end poles have significant diminished capacity. A coil located at pole 2 performed at approximately one tenth the correction capacity of the same coil located at pole 1 for the 20 cm period wiggler ends.

A second result of the modeling is that the vertical position of the correction coil on the pole has a major impact on its capacity. A coil placed on the end of the pole away from the midplane of the device produced only two fifths the correction capacity of the same coil positioned near the midplane as shown in Figure 1.



3: B_y , integral of B_y and trajectory (2nd Integral) from AMPERES calculation

Figure

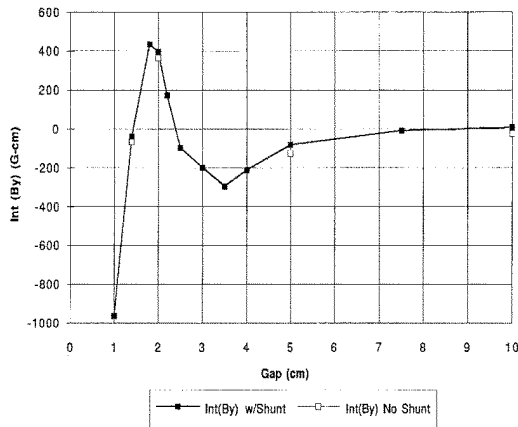


Figure 4: Gap dependency of integral of $B_y dz$

C. Gap Dependency

Extensive modeling was performed to attempt to predict the dependency of the integral of $B_y dz$ on the change in gap of the device. Figure 4 shows the results of a series of 3-D calculations for gap dependency. The indicated range of the integral from the minimum operating gap of 1.4 cm to the largest gap of 22 cm is approximately 800 G-cm.

In the 2-D modeling case the end shunt is required to achieve the necessary integral B_y capacity of correction elements. Conversely, 3-D modeling indicates that the shunt has a minimal effect on both the capacity of correctors and on the gap dependency of the integral of B_y through the ends. This can be seen in the graph of Figure 4.

D. Corrector Coil Capacity

A value of $NI = \pm 1000$ A was set for the correction coils in the models and the differences were calculated for the integrals. The indicated capacity for the 20 cm period wiggler is 5000 G-cm per end and that of the 16 cm wiggler is 4000 G-cm.

V. REFERENCES

- [1] E. Hoyer, et al, "First Undulators for the Advanced Light Source", IEEE PAC (May 1993).
- [2] E. Hoyer, et al, "Wigglers at the Advanced Light Source", IEEE PAC (May 1995).
- [3] E. Hoyer, et al, "Multiple Trim Magnet, or 'Magic Fingers', for insertion device field integral correction", 5th International Conference on Synchrotron Radiation Instrumentation, [LBL-35865], Rev. Sci. Inst. 66 (2), 1901 (February 1995).
- [4] AMPERES Three-Dimensional Magnetic Field Solver, "Users and Technical Manual", Integrated Engineering Software Inc., Winnipeg, Manitoba, Canada (1991).